UNCLASSIFIED: Distribution Statement A. Approved for public release

CHAIN DYNAMIC FORMULATIONS FOR MULTIBODY SYSTEM TRACKED VEHICLES

Michael Wallin[1]
Ahmed K. Aboubakr[1]
Paramsothy Jayakumar[2]
Michael D. Letherwood[2]
Ashraf Hamed[1]
Ahmed A. Shabana[1]

[1] Department of Mechanical and Industrial Engineering, University of Illinois at Chicago, 842 West Taylor street, Chicago, IL 60607

[2] U.S. Army TARDEC, 6501 E. 11 Mile Road, Warren, MI 48397-5000

Report Documentation Page

Form Approved
OMB No. 0704-0188

Public reporting burden for the collection of information is estimated to average 1 hour per response, including the time for reviewing instructions, searching existing data sources, gathering and maintaining the data needed, and completing and reviewing the collection of information. Send comments regarding this burden estimate or any other aspect of this collection of information, including suggestions for reducing this burden, to Washington Headquarters Services, Directorate for Information Operations and Reports, 1215 Jefferson Davis Highway, Suite 1204, Arlington VA 22202-4302. Respondents should be aware that notwithstanding any other provision of law, no person shall be subject to a penalty for failing to comply with a collection of information if it does not display a currently valid OMB control number.

1. REPORT DATE	2. REPORT TYPE	3. DATES COVERED
06 MAR 2013	**Journal Article**	**08-05-2012 to 16-02-2013**

4. TITLE AND SUBTITLE	5a. CONTRACT NUMBER
CHAIN DYNAMIC FORMULATIONS FOR MULTIBODY SYSTEM TRACKED VEHICLES	**W911NF-07-D-0001**
	5b. GRANT NUMBER
	5c. PROGRAM ELEMENT NUMBER
6. AUTHOR(S)	5d. PROJECT NUMBER
Michael Wallin; Ahmed Aboubakr; Paramsothy Jayakumar; Michael Letherwood; Ashraf Hamed	5e. TASK NUMBER
	5f. WORK UNIT NUMBER
7. PERFORMING ORGANIZATION NAME(S) AND ADDRESS(ES)	8. PERFORMING ORGANIZATION REPORT NUMBER
Department of Mechanical and Industrial Engineering,University of Illinois at Chicago,842 West Taylor Street,Chicago,IL,60607	**; #23696**
9. SPONSORING/MONITORING AGENCY NAME(S) AND ADDRESS(ES)	10. SPONSOR/MONITOR'S ACRONYM(S)
U.S. Army TARDEC, 6501 East Eleven Mile Rd, Warren, Mi, 48397-5000	**TARDEC**
	11. SPONSOR/MONITOR'S REPORT NUMBER(S)
	#23696

12. DISTRIBUTION/AVAILABILITY STATEMENT

Approved for public release; distribution unlimited

13. SUPPLEMENTARY NOTES

For JOURNAL OF NONLINEAR DYNAMICS

14. ABSTRACT

This paper is focused on the dynamic formulation of mechanical joints using different approaches that lead to different models with different numbers of degrees of freedom. Some of these formulations allow for capturing the joint deformations using discrete elastic model while the others are continuum-based and capture joint deformation modes that cannot be captured using the discrete elastic joint models. Specifically, three types of joint formulations are considered in this investigation; the ideal, compliant discrete element, and compliant continuum-based joint models. The ideal joint formulation, which does not allow for deformation degrees of freedom in the case of rigid body or small deformation analysis, requires introducing a set of algebraic constraint equations that can be handled in computational multibody system (MBS) algorithms using two fundamentally different approaches: constrained dynamics approach and penalty method. When the constrained dynamics approach is used, the constraint equations must be satisfied at the position, velocity, and acceleration levels. The penalty method, on the other hand, ensures that the algebraic equations are satisfied at the position level only. In the compliant discrete element joint formulation, no constraint conditions are used; instead the connectivity conditions between bodies are enforced using forces that can be defined in their most general form in MBS algorithms using bushing elements that allow for the definition of general nonlinear forces and moments. The new compliant continuum-based joint formulation, which is based on the finite element (FE) absolute nodal coordinate formulation (ANCF), has several advantages: (1) It captures modes of joint deformations that cannot be captured using the compliant discrete joint models; (2) It leads to linear connectivity conditions, thereby allowing for the elimination of the dependent variables at a preprocessing stage; (3) It leads to a constant inertia matrix in the case of chain like structure; and (4) It automatically captures the deformation of the bodies using distributed inertia and elasticity. The formulations of these three different joint models are compared in order to shed light on the fundamental differences between them. Numerical results of a detailed tracked vehicle model are presented in order to demonstrate the implementation of some of the formulations discussed in this investigation.

15. SUBJECT TERMS

Multibody system dynamics; joint formulations; joint compliance; penalty method; bushing elements; tracked vehicles; ANCF finite elements

16. SECURITY CLASSIFICATION OF:			17. LIMITATION OF ABSTRACT	18. NUMBER OF PAGES	19a. NAME OF RESPONSIBLE PERSON
a. REPORT	b. ABSTRACT	c. THIS PAGE			
unclassified	**unclassified**	**unclassified**	**Same as Report (SAR)**	**43**	

ABSTRACT

This paper is focused on the dynamic formulation of mechanical joints using different approaches that lead to different models with different numbers of degrees of freedom. Some of these formulations allow for capturing the joint deformations using discrete elastic model while the others are continuum-based and capture joint deformation modes that cannot be captured using the discrete elastic joint models. Specifically, three types of joint formulations are considered in this investigation; the *ideal*, *compliant discrete element*, and *compliant continuum-based joint models*. The *ideal joint formulation*, which does not allow for deformation degrees of freedom in the case of rigid body or small deformation analysis, requires introducing a set of algebraic constraint equations that can be handled in computational multibody system (MBS) algorithms using two fundamentally different approaches: constrained dynamics approach and penalty method. When the constrained dynamics approach is used, the constraint equations must be satisfied at the position, velocity, and acceleration levels. The penalty method, on the other hand, ensures that the algebraic equations are satisfied at the position level only. In the *compliant discrete element joint formulation*, no constraint conditions are used; instead the connectivity conditions between bodies are enforced using forces that can be defined in their most general form in MBS algorithms using bushing elements that allow for the definition of general nonlinear forces and moments. The new *compliant continuum-based joint formulation*, which is based on the finite element (FE) absolute nodal coordinate formulation (ANCF), has several advantages: (1) It captures modes of joint deformations that cannot be captured using the compliant discrete joint models; (2) It leads to linear connectivity conditions, thereby allowing for the elimination of the dependent variables at a preprocessing stage; (3) It leads to a constant inertia matrix in the case of chain like structure; and (4) It automatically captures the deformation of the bodies using distributed inertia and elasticity. The formulations of these three different joint models are compared in order to shed light on the fundamental differences between them. Numerical results of a detailed tracked vehicle model are presented in order to demonstrate the implementation of some of the formulations discussed in this investigation.

Keywords: Multibody system dynamics; joint formulations; joint compliance; penalty method; bushing elements; tracked vehicles; ANCF finite elements.

1. PROBLEM DEFINITION

Accurate formulation of mechanical joints is necessary in the computer simulation of multibody system (MBS) that represent many technological and industrial applications. An example of these MBS applications, in which accurate modeling of joint compliance is necessary, is the tracked vehicle shown in Fig. 1. The links of the track chains of this vehicle are connected by pin joints that can be subjected to significant stresses during the vehicle functional operations. Nonetheless, there are different joint formulations that can lead to different dynamic models which have different numbers of degrees of freedom. This study investigates the use of three different methods for formulating mechanical joints in MBS applications. These three methods are the ideal, the compliant discrete element, and the compliant continuum-based joint formulations. These three different methods are described below.

1.1 Ideal Joint Formulation

The ideal joint formulation is based on a set of algebraic equations that do not account for the joint flexibility; this is regardless of whether or not the body is flexible. The algebraic joint equations are expressed in terms of the coordinates of the two bodies connected by the joint. These algebraic equations are considered as constraint equations which can be enforced using two fundamentally different methods; the *constrained dynamics approach* and the *penalty method*. In the constrained dynamics approach, the technique of Lagrange multipliers or a recursive method is used. In this case, the joint constraint equations must be satisfied at the position, velocity, and acceleration levels. The number of degrees of freedom of the model in this case is equal to the number of the system coordinates minus the number of the algebraic joint

constraint equations. In the penalty method, on the other hand, the number of degrees of freedom of the model is not affected by the number of joint constraint equations. These joint algebraic equations are enforced using high stiffness penalty coefficients that ensure that the algebraic constraint equations are satisfied at the position level. The penalty method does not ensure that the constraint equations are satisfied at the velocity and acceleration levels.

1.2 Compliant Discrete Element Joint Formulation

In this approach, no algebraic equations are used to describe the joints between bodies in the system. The connectivity between bodies is described using force elements that have forms defined by the user of the MBS code. MBS system codes have *bushing elements* that can be used to define general linear or nonlinear force and moment expressions. The stiffness and damping coefficients in the force and moment expressions can be selected by the user. The busing elements can be used to model the joint compliance in the case of rigid and flexible body dynamics. It is important, however, to point out that adding bushing elements has no effect on the number of degrees of freedom of the model. Unlike the penalty method, the use of bushing element does not require the formulation of algebraic joint equations. Bushing elements allow for systematically introducing three force components and three moment components.

1.3 Compliant Continuum-Based Joint Formulation

The new finite element (FE) absolute nodal coordinate formulation (ANCF) allows for systematically developing new joint formulations that capture modes of deformation that cannot be captured using the discrete joint models. It also allows for modeling body flexibility using

new FE meshes that have constant inertia and linear connectivity conditions. Specifically, the compliant ANCF continuum-based joint formulation has the following advantages:

1. ANCF finite elements allow for developing new joint formulations that capture deformation modes that cannot be captured using compliant discrete joint formulations. The use of the ANCF gradient coordinates allows for developing different joint models with different numbers of degrees of freedom that allow for different strain modes.

2. The use of the ANCF gradient coordinates allows for developing linear joint constraint equations. These linear algebraic equations can be used to eliminate dependent variables at a preprocessing stage, thereby significantly reducing the model dimensionality.

3. ANCF finite elements can also be used to model the body deformation in addition to the joint compliance. Distributed inertia and elasticity are used for both body flexibility and joint compliance.

4. ANCF finite elements lead to new types of FE meshes that have constant inertia, a feature that can be exploited to develop a sparse matrix structure of the MBS dynamic equations.

It is the objective of this investigation to provide a comprehensive study of different joint formulations and demonstrate the fundamental differences between them when applied to the analysis of complex tracked vehicle system models. Simulation models of a typical tracked vehicle will be used to compare the numerical results obtained using the joint formulations discussed in this paper. These results are obtained using the general purpose MBS computer code SAMS/2000 (Shabana, 2010) which allows for systematically modeling MBS applications using the augmented formulation, penalty method, bushing elements, and ANCF finite elements. In the

augmented formulation, the technique of Lagrange multipliers is used. The computational algorithm used in SAMS/2000 ensures that the algebraic constraint equations are satisfied at the position, velocity, and acceleration levels.

2. TRACKED VEHICLES: BACKGROUND

High mobility tracked vehicle such as military battle tanks and armored personal carriers are designed for the mobility over rough and off-road terrains. Investigations on the dynamic analysis of such tracked vehicles shown in Fig. 1 have been limited because of the complexity of the forces resulting from interaction between the vehicle components. These forces are impulsive in nature, and their dynamic modeling requires sophisticated computational capabilities. Several two dimensional models for the analysis of tracked vehicle have been developed. Galaitsis (1984) demonstrated that the dynamic track tension and suspension loads in high speed tracked vehicles developed by analytical methods are useful in evaluating the dynamic characteristics of the tracked vehicle components. Bando et al. (1991) outlined a procedure for the design and analysis of rubber tracked small-size bulldozers, and presented a computer simulation which was used in the evaluation of the vehicle performance. Both steel and continuous rubber tracks are modeled by discretizing them into several rigid bodies connected by compliant elements. The simulation results indicate that the vehicle has favorable characteristics, such as less damage to the road surface, and reduced vibration and noise. Murray and Canfield (1992) used general purpose multibody computer codes to model a simple track link and sprocket system. The behavior of the interaction between the track link and the sprocket was illustrated graphically and it was found that the computer time can be significantly reduced by using supercomputers.

Nakanishi et al. (1994) developed a two dimensional contact force model for planar analysis of multibody tracked vehicle systems. Modal parameters (modal mass, modal stiffness, modal damping, and mode shapes), which are determined experimentally, are employed to simulate the nonlinear dynamic behavior of a multibody tracked vehicle which consists of interconnected rigid and flexible components. The equations of motion of the vehicle are formulated in terms of a set of modal and reference generalized coordinates, and the theoretical basis for extracting the component modal parameters of the chassis from the modal parameters of the assembled vehicle is described.

A number of approaches have been proposed in the literature for developing three-dimensional MBS models. Choi et al. (1998) developed the nonlinear dynamic equations of motion of the three-dimensional multibody tracked vehicle systems, taking into consideration the degrees of freedom of the track chains. To avoid the solution of a system of differential and algebraic equations, the recursive kinematic equations of the vehicle are expressed in terms of the independent joint coordinates. In order to take advantage of sparse matrix algorithms, the independent differential equations of the three-dimensional tracked vehicles are obtained using the velocity transformation method. Three-dimensional nonlinear contact force models that describe the interaction between the track links and the vehicle components such as the road wheels, sprockets, and idlers as well as the interaction between the track links and the ground are developed and used to define the generalized contact forces associated with the vehicle generalized coordinates. A computer simulation of a tracked vehicle in which the track is assumed to consist of track links connected by a single degree of freedom revolute joint is presented in order to demonstrate the use of the formulations presented in their study. Ryu et al.

(2000) developed compliant track link models and investigated the use of these models in the dynamic analysis of high-speed, high-mobility tracked vehicles. The characteristics of the compliant elements used in this investigation to describe the track joints are measured experimentally. A numerical integration method having a relatively large stability region is employed in order to maintain the solution accuracy, and a variable step size integration algorithm is used in order to improve the efficiency. The dimensionality problem is solved by decoupling the equations of motion of the chassis and track subsystems. Recursive methods are used to obtain a minimum set of equations for the chassis subsystem. Several simulations scenarios including an accelerated motion, high-speed motion, braking, and turning motion of the high-mobility vehicle are tested in order to demonstrate the effectiveness and validity of the methods proposed. Ozaki and Shabana (2003) evaluated the performance of different formulations using a tracked vehicle model that is subjected to impulsive forces. They developed models for joint constraints and the impulsive contact forces that result from the interaction between the track chains and the vehicle components as well as the interaction between these chains and the ground. The nonlinear contact force models used in their numerical study were developed, and the formulations of the generalized forces associated with the generalized coordinates used in each of the formulations were presented. Ryu et al (2003) investigated the nonlinear dynamic modeling methods for the virtual design of tracked vehicles by using MBS dynamic simulation techniques. The results include high oscillatory signals resulting from the impulsive contact forces and the use of stiff compliant elements to represent the joints between the track links. Each track link is modeled as a body which has six degrees of freedom, and two compliant bushing elements are used to connect track links. Efficient contact search and

kinematics algorithms in the context of the compliance contact model are developed to detect the interactions between track links, road wheels, sprockets, and ground for the sake of speedy and robust solutions. Rubinstein and Hitron (2004) developed a three-dimensional multi-body simulation model for simulating the dynamic behavior of tracked off-road vehicles using the LMS-DADS simulation program. Each track link is considered a rigid body and is connected to its neighboring track link via a revolute joint. The road-wheel track-link interaction is described using three-dimensional contact force elements, and the track-link terrain interaction is modeled using a pressure-sinkage relationship.

3. SCOPE AND OBJECTIVES OF THIS INVESTIGATION

While some of the formulations used in the analysis of tracked vehicles require the use of MBS algorithms that are designed for solving systems of differential/algebraic equations arising from kinematic joint constraints, other formulations do not require the use of such algorithms but use penalty forces or complaint elements to model the chain dynamics. The track links are subjected to high contact forces that produce high stress levels, which often cause damage to the track links during the functional operation of the vehicle. The objective of this paper is to present and compare between different joint formulations that can be used in the dynamic modeling of complex tracked vehicle systems. Better understanding of these formulations can lead to more accurate, and possibly faster, computer simulations that can be the basis for more reliable performance evaluation of the vehicles. The tracked vehicles considered in this investigation are assumed to consist of interconnected bodies that can have arbitrary displacements. In the first chain formulation, referred to in this paper as the *ideal joint chain model*, kinematic joints

between the track links are described using nonlinear constraint equations that lead to significant reduction in the number of vehicle degrees of freedom. This joint model does not require assuming stiffness and damping for the track link connectivity, and therefore, does not allow for flexibility between the tack links; it requires, however, the solution of a system of differential and algebraic equations if redundant coordinate formulations are used. Redundant coordinate algorithms based on the Lagrangian augmented form of the equations of motion require the use of Newton-Raphson method in order to ensure that the constraint equations are satisfied at the position level. Recursive and joint variables methods can also be used instead of redundant coordinate formulations in order to avoid Newton-Raphson algorithm. Another approach that can be used to enforce the constraint equations at the position level is the *penalty method*. This model does not lead to reduction in the number of the system degrees of freedom.

Two other approaches that capture the joint compliance will also be considered in this study. The first is the compliant discrete element method that employs MBS *bushing* elements to define the connectivity between the track links. This approach as in the case of the penalty method requires assuming stiffness and damping coefficients at the connection, and therefore, it allows for the flexibility between the track links. In the second, the compliant continuum-based joint formulation that employs ANCF finite elements is used. This approach, which captures new joint deformation modes, leads to linear connectivity conditions which can be applied at a preprocessing stage allowing for an efficient elimination of the dependent variables, this leads to a constant inertia matrix and zero Coriolis and centrifugal forces (Shabana et al., 2012). This approach leads to new types of FE chain meshes that have desirable characteristics.

4. ALGEBRAIC CONSTRAINT EQUATIONS

In the methods of *constrained dynamics*, there are two approaches that are often used to model ideal mechanical joints that do not account for the effect of elasticity and damping. These two methods are the *augmented formulation* that employs the technique of Lagrange multipliers or the *recursive formulation* which allows for systematic elimination of the dependent variables using the algebraic equations. These two formulations are briefly discussed in this section.

4.1 Augmented Formulation

In the augmented formulation, the constraint forces explicitly appear in the dynamic equations which are expressed in terms of redundant coordinates. The constraint relationships are used with the differential equations of motion to solve for the unknown accelerations and constraint forces. While this approach leads to a sparse matrix structure, it has the drawback of increasing the problem dimensionality and it requires more sophisticated numerical algorithms to solve the resulting system of differential and algebraic equations (DAE). Using the generalized coordinates, the equations of motion of a body i can be written as (Roberson and Schwertassek, 1988; Shabana et al., 2008)

$$\mathbf{M}^i\ddot{\mathbf{q}}^i = \mathbf{Q}_e^i + \mathbf{Q}_c^i + \mathbf{Q}_v^i \tag{1}$$

where $\mathbf{M}^i$ is the mass matrix of the body, $\ddot{\mathbf{q}}^i = \left[\ddot{\mathbf{R}}^{iT} \;\; \ddot{\boldsymbol{\theta}}^{iT}\right]^T$ is the vector of the accelerations of the body with $\mathbf{R}^i$ defining the body translation and $\boldsymbol{\theta}^i$ defining the body orientation, $\mathbf{Q}_e^i$ is the vector of external forces, $\mathbf{Q}_c^i$ is the vector of the constraint forces which can be written in terms of Lagrange multipliers $\boldsymbol{\lambda}$ as $\mathbf{Q}_c^i = -\mathbf{C}_{\mathbf{q}^i}^T\boldsymbol{\lambda}$, $\mathbf{C}_{\mathbf{q}^i}$ is the constraint Jacobian matrix associated with

the coordinates of body i, and $\mathbf{Q}_{\upsilon}^{i}$ is the vector of the inertia forces that absorb terms that are quadratic in the velocities. The constraint equations at the acceleration level can be written as $\mathbf{C}_{\mathbf{q}^i}\ddot{\mathbf{q}}^i = \mathbf{Q}_d^i$, where $\mathbf{Q}_d^i$ is a vector that absorbs first derivatives of the coordinates. Using Eq. 1 with the constraint equations at the acceleration level, one obtains

$$\begin{bmatrix} \mathbf{M} & \mathbf{C}_{\mathbf{q}}^T \\ \mathbf{C}_{\mathbf{q}} & \mathbf{0} \end{bmatrix} \begin{bmatrix} \ddot{\mathbf{q}} \\ \boldsymbol{\lambda} \end{bmatrix} = \begin{bmatrix} \mathbf{Q}_e + \mathbf{Q}_{\upsilon} \\ \mathbf{Q}_d \end{bmatrix} \tag{2}$$

The matrices and vectors that appear in this equation are the system matrices and vectors that are obtained by assembling the body matrices and vectors. The preceding matrix equation, which ensures that the constraint equations are satisfied at the acceleration level, can be solved for the accelerations and Lagrange multipliers. In order to ensure that the algebraic kinematic constraint equations are satisfied at the position and velocity levels, the independent accelerations $\ddot{\mathbf{q}}_i$ are identified and integrated forward in time in order to determine the independent velocities $\dot{\mathbf{q}}_i$ and independent coordinates $\mathbf{q}_i$. Knowing the independent coordinates from the numerical integration, the dependent coordinates $\mathbf{q}_d$ can be determined from the nonlinear constraint equations using an iterative Newton-Raphson algorithm that requires the solution of the system $\mathbf{C}_{\mathbf{q}_d}\Delta\mathbf{q}_d = -\mathbf{C}$, where $\Delta\mathbf{q}_d$ is the vector of Newton differences, and $\mathbf{C}_{\mathbf{q}_d}$ is the constraint Jacobian matrix associated with the dependent coordinates. Knowing the system coordinates and the independent velocities, the dependent velocities $\dot{\mathbf{q}}_d$ can be determined by solving a linear system of algebraic equations that represents the constraint equations at the velocity level. This linear system of equations in the velocities can be written as $\mathbf{C}_{\mathbf{q}_d}\dot{\mathbf{q}}_d = -\mathbf{C}_{\mathbf{q}_i}\dot{\mathbf{q}}_i - \mathbf{C}_t$; where $\mathbf{C}_{\mathbf{q}_i}$ is

the constraint Jacobian matrix associated with the independent coordinates, and $\mathbf{C}_t = \partial \mathbf{C}/\partial t$ is the partial derivative of the constraint functions with respect to time.

Lagrange multipliers, on the other hand, can be used to determine the constraint forces. For a given joint k, the generalized constraint forces acting on body i, connected by this joint, can be obtained from the equation

$$\left(\mathbf{Q}_c^i\right)_k = -\left(\mathbf{C}_k\right)_{\mathbf{q}^i}^T \boldsymbol{\lambda}_k = \begin{bmatrix} \mathbf{F}_k^{iT} & \mathbf{T}_k^{iT} \end{bmatrix}^T \tag{3}$$

Where $\mathbf{F}_k^i$ and $\mathbf{T}_k^i$ are the generalized joint forces associated, respectively, with the translation and orientation coordinates of body i. Using the results of Eq. 3, the reaction forces at the joint definition point can be determined using the concept of the equipollent systems of forces.

4.2 Recursive Formulation

Another alternate approach for formulating the equations of motion of constrained mechanical systems is the recursive method, wherein the equations of motion are formulated in terms of the joint degrees of freedom. This formulation leads to a minimum set of differential equations from which the workless constraint forces are automatically eliminated (Roberson and Schwertassek, 1988; Shabana, 2010). The numerical procedure used in solving these differential equations is much simpler than the procedure used in the solution of the mixed system of differential and algebraic equations resulting from the use of the augmented formulation. In the recursive formulation, the equations of motion are formulated in terms of joint degrees of freedom. In this formulation, the multibody system is assumed to consist of subsystems, as in the case of the track chains shown in Fig. 2. The absolute coordinates and velocities of an arbitrary body i in a

subsystem are expressed in terms of the independent joint variables as well as the absolute coordinates and velocities of body j. If body i is connected to body j through a revolute joint, which is the case in this subsystem, the relative rotation is the only degree of freedom represented between the bodies. The connectivity between bodies i and body j can then be described using the kinematic relationships

$$\left.\begin{aligned} &\mathbf{R}^i + \mathbf{A}^i\bar{\mathbf{u}}_P^i - \mathbf{R}^j - \mathbf{A}^j\bar{\mathbf{u}}_P^j = \mathbf{0} \\ &\boldsymbol{\omega}^i = \boldsymbol{\omega}^j + \boldsymbol{\omega}^{i,j} \end{aligned}\right\} \tag{4}$$

where $\mathbf{R}^i$ is the global position vector of the origin of body *i*; $\mathbf{A}^i$ is the transformation matrix that defines the body orientation and can be expressed in terms of Euler parameters; $\bar{\mathbf{u}}_P^i$ and $\bar{\mathbf{u}}_P^j$ are the local position vectors of point P defined in the coordinate systems of body *i* and j, respectively, $\boldsymbol{\omega}^i$ and $\boldsymbol{\omega}^j$ are, respectively, the absolute angular velocity vectors of bodies *i* and j, and $\boldsymbol{\omega}^{i,j}$ is the angular velocity vector of body *i* with respect to body j which can be defined as $\boldsymbol{\omega}^{i,j} = \dot{\phi}^i\mathbf{v}^j$, with $\mathbf{v}^j = \mathbf{A}^j\bar{\mathbf{v}}^j$ where $\bar{\mathbf{v}}^j$ is a unit vector along the axis of rotation defined in the coordinate system of body j, and ϕ^i is the angle of relative rotation. By differentiating the first equation in Eq. 4 twice and the second once with respect to time, one obtains

$$\left.\begin{aligned} &\ddot{\mathbf{R}}^i = -\boldsymbol{\omega}^i\times(\boldsymbol{\omega}^i\times\mathbf{u}_P^i) - \boldsymbol{\alpha}^i\times\mathbf{u}_P^i + \ddot{\mathbf{R}}^j + \boldsymbol{\omega}^j\times(\boldsymbol{\omega}^j\times\mathbf{u}_P^j) + \boldsymbol{\alpha}^j\times\mathbf{u}_P^j \\ &\boldsymbol{\alpha}^i = \boldsymbol{\alpha}^j + \mathbf{v}^j\ddot{\phi}^i + (\boldsymbol{\omega}^j\times\mathbf{v}^j)\dot{\phi}^i \end{aligned}\right\} \tag{5}$$

In this equation, $\boldsymbol{\alpha}^k$ is the absolute angular acceleration vector of body k. Using the kinematic equations obtained in this section, one can systematically eliminate the dependent variables in order to obtain a number of differential equations of motion equal to the number of the system

degrees of freedom. Using this approach, one obtains a dense inertia matrix in a system of dynamic equations that does not have constraint forces. A second, alternative approach is to use the kinematic equations developed in this section to determine all the system absolute coordinates and velocities. One can then construct Eq. 2, which can be solved for the accelerations and Lagrange multipliers. Using the absolute acceleration relationships of Eq. 5, one can determine the relative joint accelerations. The joint accelerations can be integrated forward in time in order to determine the joint coordinates and velocities.

5. GENERALIZED FORCES

In defining the joint forces between the track links, it is important to understand the relationship and differences between the generalized and the Cartesian moments (Roberson and Schwertassek, 1988; Shabana, 2010). This is important in interpreting the reaction forces of the ideal joints and also important in the implementation of the penalty method and bushing elements. Let $\mathbf{F}^i$ be a force vector that acts at a point P^i on a rigid body *i*. If this force vector is assumed to be defined in the global coordinate system, then the virtual work of this force vector can be written as $\delta W_e^i = \mathbf{F}^{i^T} \delta \mathbf{r}_P^i$, where $\delta \mathbf{r}_P^i$ can be found using the virtual change in the position vector of an arbitrary point on rigid body i as

$$\delta \mathbf{r}_P^i = \begin{bmatrix} \mathbf{I} & -\mathbf{A}^i \tilde{\bar{\mathbf{u}}}_P^i \bar{\mathbf{G}}^i \end{bmatrix} \begin{bmatrix} \delta \mathbf{R}^i \\ \delta \boldsymbol{\theta}^i \end{bmatrix} \tag{6}$$

In this equation, $\mathbf{A}^i$ is the transformation matrix that defines the body orientation, $\tilde{\bar{\mathbf{u}}}_P^i$ is the skew symmetric matrix associated with the vector $\bar{\mathbf{u}}_P^i$ that defines the local coordinates of the point

P^i, and $\bar{\mathbf{G}}^i$ is the matrix that relates the angular velocity vector $\bar{\boldsymbol{\omega}}^i$ defined in the body coordinate system to the time derivatives of the orientation coordinates, that is $\bar{\boldsymbol{\omega}}^i = \bar{\mathbf{G}}^i \dot{\boldsymbol{\theta}}^i$. Note that since $\tilde{\mathbf{u}}_P^i = \mathbf{A}^i \tilde{\bar{\mathbf{u}}}_P^i \mathbf{A}^{i^T}$, Eq. 6 can be written as $\delta \mathbf{r}_P^i = \delta \mathbf{R}^i - \tilde{\mathbf{u}}_P^i \mathbf{G}^i \delta \boldsymbol{\theta}^i$. Using this equation in the virtual work expression, one obtains $\delta W_e^i = \mathbf{F}^{i^T} \delta \mathbf{R}^i - \mathbf{F}^{i^T} \tilde{\mathbf{u}}_P^i \mathbf{G}^i \delta \boldsymbol{\theta}^i$, which can be written as

$$\delta W_e^i = \mathbf{F}_R^{i^T} \delta \mathbf{R}^i + \mathbf{F}_\theta^{i^T} \delta \boldsymbol{\theta}^i \tag{7}$$

where $\mathbf{F}_R^i = \mathbf{F}^i$, and $\mathbf{F}_\theta^i = -\mathbf{G}^{i^T} \tilde{\mathbf{u}}_P^{i^T} \mathbf{F}^i$. These equations imply that a force that acts at an arbitrary point on the rigid body *i* is equipollent to another system defined at the reference point that consists of the same force and a set of generalized forces, defined by $\mathbf{F}_\theta^i = -\mathbf{G}^{i^T} \tilde{\mathbf{u}}_P^{i^T} \mathbf{F}^i$ associated with the orientation coordinates of the body (Roberson and Schwertassek, 1988; Shabana, 2010).

Since $\tilde{\mathbf{u}}_P^i$ is a skew-symmetric matrix, it follows that $\tilde{\mathbf{u}}_P^i = -\tilde{\mathbf{u}}_P^{i^T}$. Using this identity, one can show that the generalized moment can be written as $\mathbf{F}_\theta^i = \mathbf{G}^{i^T} (\mathbf{u}_P^i \times \mathbf{F}^i)$, where $\mathbf{M}_a^i = \mathbf{u}_P^i \times \mathbf{F}^i$ is the Cartesian moment resulting from the application of the force $\mathbf{F}^i$, and $\mathbf{G}^i$ is the matrix that relates the angular velocity vector $\boldsymbol{\omega}^i$ defined in the global coordinate system to the time derivatives of the orientation coordinates, that is $\boldsymbol{\omega}^i = \mathbf{G}^i \dot{\boldsymbol{\theta}}^i$. It follows that the relationship between the generalized and Cartesian moment is $\mathbf{F}_\theta^i = \mathbf{G}^{i^T} \mathbf{M}_a^i$. If the components of the moment vector are defined in the body coordinate system, one has $\mathbf{F}_\theta^i = \bar{\mathbf{G}}^{i^T} \bar{\mathbf{M}}_a^i$, where $\bar{\mathbf{M}}_a^i = \mathbf{A}^{i^T} \mathbf{M}_a^i$. The relationships developed in this section will be used in the formulation of

the joint forces in the case of the penalty method. These relationships will also be used in the computer implementation of the bushing element in general MBS algorithms.

6. JOINT FORMULATIONS

In this paper, four different joint models are considered; two models are based on algebraic equations that require the use of the methods of constrained dynamics or the penalty method. In the case of constrained dynamics, an alternative to the use of Lagrange multipliers is the use of the recursive methods, as previously discussed. When Lagrange multiplier technique or the recursive methods are used, the constraint equations must be satisfied at the position, velocity, and acceleration levels. The penalty method, on the other hand, satisfies the algebraic constraint equations at the position level only.

6.1 Constraint Equations

The revolute (pin) joint is used in this section as an example to demonstrate the formulation of the algebraic constraint equations. This joint has been used in the literature in the modeling of the track chains. As shown in Fig. 2, the track chain can be assumed to consist of links connected to each other by a pin joint that allows for the relative rotation between them. In general MBS algorithms, the nonlinear algebraic equations that define the pin joint are expressed in terms of the absolute coordinates of the two bodies i and j connected by the joint. The five algebraic constraint equations that eliminate five degrees of freedom can be written in terms of the absolute Cartesian coordinates of the two bodies as (Shabana, 2010)

$$\mathbf{C}\left(\mathbf{q}^i,\mathbf{q}^j\right)=\left[\mathbf{v}_1^{iT}\mathbf{v}^j \quad \mathbf{v}_2^{iT}\mathbf{v}^j \quad \mathbf{v}_1^{iT}\mathbf{r}_P^{ij} \quad \mathbf{v}_2^{iT}\mathbf{r}_P^{ij} \quad \mathbf{r}_P^{ijT}\mathbf{r}_P^{ij}-k_\theta\right]^T=\mathbf{0} \tag{8}$$

where $\mathbf{v}^i$ and $\mathbf{v}^j$ are two vectors defined along the joint axis on bodies i and j, respectively; $\mathbf{v}^i,\mathbf{v}_1^i,\mathbf{v}_2^i$ form an orthogonal triad defined on body i; k_θ is a constant (Shabana, 2010); and

$$\mathbf{r}_P^{ij}=\mathbf{r}_P^i-\mathbf{r}_P^j=\mathbf{R}^i+\mathbf{A}^i\bar{\mathbf{u}}_P^i-\mathbf{R}^j-\mathbf{A}^j\bar{\mathbf{u}}_P^j \tag{9}$$

In this equation, $\mathbf{A}^i$ and $\mathbf{A}^j$ are the transformation matrices that define the orientation of bodies i and j, respectively, and $\bar{\mathbf{u}}_P^i$ and $\bar{\mathbf{u}}_P^j$ are the local position vectors of points P^i and P^j with respect to bodies i and j, respectively. Points P^i and P^j are defined on the axis of the pin joint on bodies i and j, respectively. One can show that the Jacobian matrix of the pin joint constraints is defined as

$$\mathbf{C}_\mathbf{q}=\left[\mathbf{C}_{\mathbf{q}^i} \quad \mathbf{C}_{\mathbf{q}^j}\right]=\begin{bmatrix}\mathbf{v}^{jT}\mathbf{H}_1^i & \mathbf{v}_1^{iT}\mathbf{H}^j\\ \mathbf{v}^{jT}\mathbf{H}_2^i & \mathbf{v}_2^{iT}\mathbf{H}^j\\ \mathbf{r}_P^{ijT}\mathbf{H}_1^i+\mathbf{v}_1^{iT}\mathbf{H}_P^i & -\mathbf{v}_1^{iT}\mathbf{H}_P^j\\ \mathbf{r}_P^{ijT}\mathbf{H}_2^i+\mathbf{v}_2^{iT}\mathbf{H}_P^i & -\mathbf{v}_2^{iT}\mathbf{H}_P^j\\ 2\mathbf{r}_P^{ijT}\mathbf{H}_P^i & -2\mathbf{r}_P^{ijT}\mathbf{H}_P^j\end{bmatrix} \tag{10}$$

where $\mathbf{C}_{\mathbf{q}^i}$ and $\mathbf{C}_{\mathbf{q}^j}$ are the constraint Jacobian matrices associated with the coordinates of bodies i and j, respectively; and other vectors and matrices that appear in the preceding equation are

$$\mathbf{H}_P^i=\left[\mathbf{I} \quad \mathbf{A}^i\tilde{\bar{\mathbf{u}}}_P^{iT}\bar{\mathbf{G}}^i\right],\ \mathbf{H}_P^j=\left[\mathbf{I} \quad \mathbf{A}^j\tilde{\bar{\mathbf{u}}}_P^{jT}\bar{\mathbf{G}}^j\right],\ \mathbf{H}_1^i=\frac{\partial\mathbf{v}_1^i}{\partial\mathbf{q}^i}=\frac{\partial}{\partial\mathbf{q}^i}\left(\mathbf{A}^i\bar{\mathbf{v}}_1^i\right),\ \mathbf{H}_2^i=\frac{\partial\mathbf{v}_2^i}{\partial\mathbf{q}^i}=\frac{\partial}{\partial\mathbf{q}^i}\left(\mathbf{A}^i\bar{\mathbf{v}}_2^i\right),$$

$$\mathbf{H}^j=\frac{\partial\mathbf{v}^j}{\partial\mathbf{q}^j}=\frac{\partial}{\partial\mathbf{q}^j}\left(\mathbf{A}^j\bar{\mathbf{v}}^j\right).$$

Another alternate approach for formulating the revolute joint constraints is to consider it as a special case of the spherical joint in which the relative rotation between the two bodies is allowed only along the joint axis. If point P is the joint definition point, and $\mathbf{v}^i$ and $\mathbf{v}^j$ are two vectors defined along the joint axis on bodies i and j, respectively, the constraint equations of the revolute joint can be written as $\mathbf{C}\left(\mathbf{q}^i, \mathbf{q}^j\right) = \begin{bmatrix} \mathbf{r}_P^{ij} & \mathbf{v}_1^{iT}\mathbf{v}^j & \mathbf{v}_2^{iT}\mathbf{v}^j \end{bmatrix}^T = \mathbf{0}$. The last two equations in this equation guarantee that the two vectors $\mathbf{v}^i$ and $\mathbf{v}^j$ remain parallel, thereby eliminating the freedom of the relative rotation between the two bodies in two perpendicular directions.

6.2 Penalty Method

The constraint equations that describe the connectivity between the track links can be enforced using the penalty approach. In this case, these algebraic equations are satisfied only at the position level. The penalty method does not lead to elimination of degrees of freedom, and therefore, it is conceptually different from the case of Lagrange multiplier technique or the recursive approach. In order to demonstrate the penalty approach, the violations in the constraint equations of a revolute joint k can be written as

$$\mathbf{d}_k = \begin{bmatrix} \mathbf{r}_P^{ij} & \mathbf{v}_1^{iT}\mathbf{v}^j & \mathbf{v}_2^{iT}\mathbf{v}^j \end{bmatrix}^T \tag{11}$$

Using this violation $\mathbf{d}_k$, a restoring force vector can then be defined as $\mathbf{f}_k = k_k \mathbf{d}_k + c_k \dot{\mathbf{d}}_k$, where k_k, and c_k are assumed penalty stiffness and damping coefficients, respectively, and $\dot{\mathbf{d}}_k$ is the time derivative of the violation vector $\mathbf{d}_k$. The virtual work of this restoring force $\mathbf{f}_k$ can then be written as $\delta W_k^{ij} = -\mathbf{f}_k{}^T \delta \mathbf{d}_k$, which can be written as

$$\delta W_k^{ij} = -\mathbf{F}_B^T \delta \mathbf{r}_p^{ij} - F_1 \delta\left(\mathbf{v}_1^{iT}\mathbf{v}^j\right) - F_2 \delta\left(\mathbf{v}_2^{iT}\mathbf{v}^j\right) \tag{12}$$

where $\delta \mathbf{r}_p^{ij} = \delta \mathbf{R}^i - \tilde{\mathbf{u}}_P^i \mathbf{G}^i \delta \boldsymbol{\theta}^i - \delta \mathbf{R}^j + \tilde{\mathbf{u}}_P^j \mathbf{G}^j \delta \boldsymbol{\theta}^j$, $\mathbf{F}_B = k_k \mathbf{r}_p^{ij} + c_k \dot{\mathbf{r}}_p^{ij}$, $\delta(\mathbf{v}_1^{iT}\mathbf{v}^j) = \mathbf{v}^{jT}\delta\mathbf{v}_1^i + \mathbf{v}_1^{iT}\delta\mathbf{v}^j$,

$\delta(\mathbf{v}_2^{iT}\mathbf{v}^j) = \mathbf{v}^{jT}\delta\mathbf{v}_2^i + \mathbf{v}_2^{iT}\delta\mathbf{v}^j$, $F_1 = k_k\left(\mathbf{v}_1^{iT}\mathbf{v}^j\right) + c_k \dfrac{d\left(\mathbf{v}_1^{iT}\mathbf{v}^j\right)}{dt}$, and $F_2 = k_k\left(\mathbf{v}_2^{iT}\mathbf{v}^j\right) + c_k \dfrac{d\left(\mathbf{v}_2^{iT}\mathbf{v}^j\right)}{dt}$.

Equation 12 can be used to define a set of generalized forces acting on bodies *i* and *j* that maintain the connectivity between the two bodies as

$$\delta W_k^{ij} = \mathbf{Q}_R^{iT}\delta\mathbf{R}^i + \mathbf{Q}_\theta^{iT}\delta\boldsymbol{\theta}^i + \mathbf{Q}_R^{jT}\delta\mathbf{R}^j + \mathbf{Q}_\theta^{jT}\delta\boldsymbol{\theta}^j \tag{13}$$

Which can be rewritten in a compact form as $\delta W = \mathbf{Q}_B^{iT}\delta\mathbf{q}^i + \mathbf{Q}_B^{jT}\delta\mathbf{q}^j$, where $\mathbf{q}^i$ and $\mathbf{q}^j$ are the generalized coordinates of bodies i and j, and

$$\left.\begin{aligned} \mathbf{Q}_B^i &= \begin{bmatrix} \mathbf{Q}_R^i \\ \mathbf{Q}_\theta^i \end{bmatrix} = \begin{bmatrix} -\mathbf{F}_B \\ \mathbf{G}^{iT}\tilde{\mathbf{u}}_P^{iT}\mathbf{F}_B + \mathbf{G}^{iT}\mathbf{M}_1^i + \mathbf{G}^{iT}\mathbf{M}_2^i \end{bmatrix} \\ \mathbf{Q}_B^j &= \begin{bmatrix} \mathbf{Q}_R^j \\ \mathbf{Q}_\theta^j \end{bmatrix} = \begin{bmatrix} \mathbf{F}_B \\ -\mathbf{G}^{jT}\tilde{\mathbf{u}}_P^{jT}\mathbf{F}_B - \mathbf{G}^{jT}\mathbf{M}_1^i - \mathbf{G}^{jT}\mathbf{M}_2^i \end{bmatrix} \end{aligned}\right\} \tag{14}$$

where $\mathbf{M}_1^i = -F_1\tilde{\mathbf{v}}_1^i\mathbf{v}^j$, $\mathbf{M}_1^j = F_1\tilde{\mathbf{v}}_1^i\,\mathbf{v}^j$, $\mathbf{M}_2^i = -F_1\tilde{\mathbf{v}}_2^i\,\mathbf{v}^j$, and $\mathbf{M}_2^j = F_1\tilde{\mathbf{v}}_2^i\,\mathbf{v}^j$. Equation 14 defines the generalized forces associated with the absolute Cartesian coordinates due to the revolute joint connection between bodies i and j. With a proper selection of the penalty coefficients, these forces ensure that the constraint equations are satisfied at the position level.

7. COMPLIANT DISCRETE ELEMENT JOINT FORMULATION

The compliant discrete element joint formulation allows for introducing joint deformations. In this approach, no algebraic equations are enforced. In most MBS computer codes, the compliant discrete element joint method can be applied using the standard MBS bushing element that allows for introducing three force and three moment components that can be linear or nonlinear functions of the body coordinates. As shown in Fig. 3, the position vectors $\bar{\mathbf{u}}_{P_1}^j$ and $\bar{\mathbf{u}}_{P_2}^j$ of two points, P_1^j and P_2^j on body *j*, can be used to define one axis of the coordinate system of the bushing element as $\bar{\mathbf{n}}^j = \left(\bar{\mathbf{u}}_{p_1}^j - \bar{\mathbf{u}}_{p_2}^j\right) \Big/ \left|\bar{\mathbf{u}}_{p_1}^j - \bar{\mathbf{u}}_{p_2}^j\right|$, where $\bar{\mathbf{n}}^j$ is one of the bushing axes defined in the body j coordinate system. This axis can then be defined in the global coordinate system as $\mathbf{n}^j = \mathbf{A}^j \bar{\mathbf{n}}^j$, where $\mathbf{A}^j$ is the transformation matrix that defines the orientation of the coordinate system of body j in the global system. Using this axis, one can define the directional properties of the bushing element with the other two axes of the bushing coordinate system being defined using the transformation matrix $\bar{\mathbf{A}}^{bj} = \left[\bar{\mathbf{t}}_1^j \quad \bar{\mathbf{t}}_2^j \quad \bar{\mathbf{n}}^j\right]$ where $\bar{\mathbf{t}}_1^j$ and $\bar{\mathbf{t}}_2^j$ are the two unit vectors that complete the three orthogonal axes of the bushing element coordinate system. Assuming that body j is a rigid body, the bushing coordinate system can be defined with respect to the global coordinate system as $\mathbf{A}^{bj} = \mathbf{A}^j \bar{\mathbf{A}}^{bj}$. Choosing points P^i and P_1^j to initially coincide; one can define the bushing deformation and rate of deformation vectors in the bushing coordinate system as $\bar{\boldsymbol{\delta}}^{bij} = \mathbf{A}^{bj^T} \mathbf{r}^{ij}$, and $\dot{\bar{\boldsymbol{\delta}}}^{bij} = \mathbf{A}^{bj^T} \dot{\mathbf{r}}^{ij}$, respectively, where $\mathbf{r}^{ij} = \mathbf{r}_P^i - \mathbf{r}_{P_1}^j$ is the position vector of point P_1^j with respect to point P^i.

The rotational deformation of the bushing element can be obtained using the transformation matrix that defines the orientation of the bushing coordinate system on body i with respect to the

bushing coordinate system on body j. This matrix is defined as $\mathbf{A}^{bij} = \mathbf{A}^{bj^T}\mathbf{A}^{bi}$, where $\mathbf{A}^{bj}$ is the orientation matrix of the bushing coordinate system on body j, while $\mathbf{A}^{bi}$ is the orientation matrix of the bushing coordinate system with respect to the coordinate system of body i that is defined as $\mathbf{A}^{bi} = \mathbf{A}^{i}\overline{\mathbf{A}}^{bi}$. Assuming that the relative rotations between bodies i and j are small, the relative rotation matrix, $\mathbf{A}^{bij}$ can be used to extract three relative rotations defined in the bushing coordinate system, $\overline{\boldsymbol{\theta}}^{bij} = \left[\theta_x^{bij} \quad \theta_y^{bij} \quad \theta_z^{bij}\right]^T$. The relative angular velocity between the two bodies defined in the bushing coordinate system can also be written as $\overline{\boldsymbol{\omega}}^{bij} = \mathbf{A}^{bj^T}(\boldsymbol{\omega}^i - \boldsymbol{\omega}^j)$, where $\boldsymbol{\omega}^i$ and $\boldsymbol{\omega}^j$ are the absolute angular velocity vectors of bodies i and j, respectively, defined in the global coordinate system. The bushing stiffness and damping coefficients are often determined using experimental testing, and these coefficients are defined generally in the bushing coordinate system. Let $\mathbf{K}_r$ and $\mathbf{C}_r$ be the translational stiffness and damping matrices, respectively, defined with respect to the bushing coordinate system; and assume that the rotational stiffness and damping matrices are $\mathbf{K}_\theta$ and $\mathbf{C}_\theta$, respectively. In terms of translational and rotational stiffness and damping matrices, the force vector defined in the bushing coordinate system can be written as

$$\begin{bmatrix} \overline{\mathbf{F}}_R^b \\ \overline{\mathbf{M}}_\theta^b \end{bmatrix} = \begin{bmatrix} \mathbf{K}_r & \mathbf{0} \\ \mathbf{0} & \mathbf{K}_\theta \end{bmatrix} \begin{bmatrix} \overline{\boldsymbol{\delta}}^{bij} \\ \overline{\boldsymbol{\theta}}^{bij} \end{bmatrix} + \begin{bmatrix} \mathbf{C}_r & \mathbf{0} \\ \mathbf{0} & \mathbf{C}_\theta \end{bmatrix} \begin{bmatrix} \dot{\overline{\boldsymbol{\delta}}}^{bij} \\ \overline{\boldsymbol{\omega}}^{bij} \end{bmatrix} \tag{15}$$

This force vector can then be defined in the global coordinate system, and the results can be used to define the generalized bushing forces and moments acting on the two bodies as previously described in this paper.

8. COMPLIANT CONTINUUM-BASED JOINT FORMULATION

The compliant continuum-based joint formulation allows capturing joint strain modes that cannot be captured using the compliant discrete element joint method. When ANCF finite elements are used, one can develop new FE meshes that have linear connectivity and constant inertia (Shabana et al., 2012). This allows for systematically eliminating dependent variables at a preprocessing stage, and as a result, there is no need for the use of joint formulations in the main processor. This approach can be used to develop new spatial chain models where the modes of deformations at the definition points of the joints that allow for rigid body rotations between ANCF finite elements can be captured. The displacement field of an ANCF finite element, as the one shown in Fig. 4, can be written as $\mathbf{r}(x,y,z,t)=\mathbf{s}(x,y,z)\mathbf{e}(t)$ where x, y, and z are the element spatial coordinates; t is time; $\mathbf{S}$ is the element shape function matrix, and $\mathbf{e}$ is the vector of element nodal coordinates. Using this displacement field, the equations of a pin joint between elements i and j can be written using the six scalar equations $\mathbf{r}^i=\mathbf{r}^j, \mathbf{r}_\alpha^i=\mathbf{r}_\alpha^j$, where α is the coordinate line that defines the joint axis; α can be x, y, or z or any other coordinate line. The six scalar equations eliminate six degrees of freedom; three translations, two rotations, and one deformation mode. Therefore, this joint has five modes of deformation that include stretch and shear modes. This ANCF revolute joint model ensures C^1 continuity with respect to the coordinate line α and C^0 continuity with respect to the other two parameters. It follows that the Lagrangian strain component $\varepsilon_{\alpha\alpha}=\left(\mathbf{r}_\alpha^T\mathbf{r}_\alpha-1\right)\big/2$ is continuous at the joint definition point, while the other five strain components can be discontinuous. The resulting joint constraint equations are linear, and therefore, can be applied at a preprocessing stage to systematically eliminate the dependent variables. Using these equations, one can develop a new kinematically

linear FE mesh for flexible-link chains in which the links can have arbitrarily large relative rotations.

In the numerical investigation presented in this paper, a three-dimensional cable element is used to model the flexibility of the chain links. For the three-dimensional cable element used in the compliant continuum-based model, the nodal coordinates can be written as $\mathbf{e}^j = \left[\mathbf{r}^{j^T}(x_1^j = 0) \quad \mathbf{r}_{x_1}^{j^T}(x_1^j = 0) \quad \mathbf{r}^{j^T}(x_1^j = l) \quad \mathbf{r}_{x_1}^{j^T}(x_1^j = l)\right]^T$, with the element shape function defined as $\mathbf{S}^j = \left[s_1\mathbf{I} \quad s_2\mathbf{I} \quad s_3\mathbf{I} \quad s_4\mathbf{I}\right]$ where $\mathbf{I}$ is the 2×2 identity matrix (Gerstmayr and Shabana, 2006). The shape functions s_i, for i = 1, 2, 3, 4, are defined as

$$\begin{aligned} s_1 &= 1 - 3\xi^2 + 2\xi^3, \quad s_2 = l(\xi - 2\xi^2 + \xi^3), \\ s_3 &= \quad 3\xi^2 - 2\xi^3, \quad s_4 = l(-\xi^2 + \xi^3), \end{aligned} \tag{16}$$

where $\xi = x_1^j / l$ and l is the length of the element. The constraint forces, $\mathbf{Q}_C^j$, can then be found using the equation of motion for a single body (element) j as $\mathbf{M}^j\ddot{\mathbf{e}}^j = (\mathbf{Q}_s^j + \mathbf{Q}_{con}^j + \mathbf{Q}_e^j) + \mathbf{Q}_C^j$, where $\mathbf{Q}_s^j$, $\mathbf{Q}_{con}^j$, and $\mathbf{Q}_e^j$ are the elastic forces, forces of contacts between the chain links and other bodies in the system, and gravity forces, respectively, associated with the element nodal coordinates $\mathbf{e}^j$ and $\mathbf{M}^j$ is the symmetric mass matrix of the finite element j defined as $\mathbf{M}^j = \int_{V^j} \rho^j \mathbf{S}^{j^T} \mathbf{S}^j dV^j$, where ρ^j is the mass density of the material points of the element and V^j is the element volume. Since the shape function for a three-dimensional cable element only depends on the x_1 spatial coordinate, the mass matrix can then be defined as

$$\mathbf{M}^j = \int_{\frac{-d}{2}}^{\frac{d}{2}} \int_{\frac{-h}{2}}^{\frac{h}{2}} \int_0^l \rho_0^j \mathbf{S}^{j^T} \mathbf{S}^j dx_1 dx_2 dx_3 = d^j h^j \rho_0^j \int_0^l \mathbf{S}^{j^T} \mathbf{S}^j dx_1 \tag{17}$$

For the cable element, this mass matrix can be written explicitly as

$$\mathbf{M}^j = d^j h^j \rho_0^j \begin{bmatrix}
\frac{13}{35}l & 0 & 0 & \frac{11}{210}l^2 & 0 & 0 & \frac{9}{70}l & 0 & 0 & -\frac{13}{420}l^2 & 0 & 0 \\
0 & \frac{13}{35}l & 0 & 0 & \frac{11}{210}l^2 & 0 & 0 & \frac{9}{70}l & 0 & 0 & -\frac{13}{420}l^2 & 0 \\
0 & 0 & \frac{13}{35}l & 0 & 0 & \frac{11}{210}l^2 & 0 & 0 & \frac{9}{70}l & 0 & 0 & -\frac{13}{420}l^2 \\
\frac{11}{210}l^2 & 0 & 0 & \frac{1}{105}l^3 & 0 & 0 & \frac{13}{420}l^2 & 0 & 0 & -\frac{1}{140}l^3 & 0 & 0 \\
0 & \frac{11}{210}l^2 & 0 & 0 & \frac{1}{105}l^3 & 0 & 0 & \frac{13}{420}l^2 & 0 & 0 & -\frac{1}{140}l^3 & 0 \\
0 & 0 & \frac{11}{210}l^2 & 0 & 0 & \frac{1}{105}l^3 & 0 & 0 & \frac{13}{420}l^2 & 0 & 0 & -\frac{1}{140}l^3 \\
\frac{9}{70}l & 0 & 0 & \frac{13}{420}l^2 & 0 & 0 & \frac{13}{35}l & 0 & 0 & -\frac{11}{210}l^2 & 0 & 0 \\
0 & \frac{9}{70}l & 0 & 0 & \frac{13}{420}l^2 & 0 & 0 & \frac{13}{35}l & 0 & 0 & -\frac{11}{210}l^2 & 0 \\
0 & 0 & \frac{9}{70}l & 0 & 0 & \frac{13}{420}l^2 & 0 & 0 & \frac{13}{35}l & 0 & 0 & -\frac{11}{210}l^2 \\
-\frac{13}{420}l^2 & 0 & 0 & -\frac{1}{140}l^3 & 0 & 0 & -\frac{11}{210}l^2 & 0 & 0 & \frac{1}{105}l^3 & 0 & 0 \\
0 & -\frac{13}{420}l^2 & 0 & 0 & -\frac{1}{140}l^3 & 0 & 0 & -\frac{11}{210}l^2 & 0 & 0 & \frac{1}{105}l^3 & 0 \\
0 & 0 & -\frac{13}{420}l^2 & 0 & 0 & -\frac{1}{140}l^3 & 0 & 0 & -\frac{11}{210}l^2 & 0 & 0 & \frac{1}{105}l^3
\end{bmatrix} \tag{18}$$

where d^j, h^j, and ρ_0^j are the width, height, and initial density, respectively, of element *j*. It is important to note that the mass matrix is constant in both two-dimensional and three-dimensional cases and leads to zero centrifugal and Coriolis forces when the body experiences an arbitrary large deformation and finite rotation. The virtual work of the elastic forces can then be defined as

$$\delta W_s = \int_0^l EA\varepsilon_{11}\delta\varepsilon_{11} dx_1 + \int_0^l EI\kappa\delta\kappa dx_1 \tag{19}$$

where E is the modulus of elasticity, A is the element cross section, I is the second moment of area and κ is the curvature. The elastic forces of the cable element can also be evaluated using

the following expression for the strain energy $U = \int_0^l EA(\varepsilon_{11})^2 dx_1 + \int_0^l EI(\kappa)^2 dx_1$ as $\mathbf{Q}_s = \left(\frac{\partial U}{\partial \mathbf{e}}\right)^T$.

Similarly, the gravity forces can be found using the virtual work of the gravity forces, $\delta W_e = \int_V [0 \quad 0 \quad -\rho_0 g]\mathbf{S}\delta\mathbf{e}dV$. Substituting in the shape functions and integrating over the volume leads to $\delta W_s = -mg\left[0 \quad 0 \quad \frac{1}{2} \quad 0 \quad 0 \quad \frac{l}{12} \quad 0 \quad 0 \quad \frac{1}{2} \quad 0 \quad 0 \quad \frac{-l}{12}\right]\delta\mathbf{e}$, which leads to

$$\mathbf{Q}_e = -mg\left[0 \quad 0 \quad \frac{1}{2} \quad 0 \quad 0 \quad \frac{l}{12} \quad 0 \quad 0 \quad \frac{1}{2} \quad 0 \quad 0 \quad \frac{-l}{12}\right] \tag{20}$$

Using the principle of virtual work with the mass matrix and nodal accelerations as previously defined, the joint forces for a specific element can then be easily calculated.

9. SIMULATION RESULTS

In this section, numerical results, obtained using the tracked vehicle model shown in Fig. 1, are used to compare the different joint formulations presented in this investigation. The tracked vehicle modeled is an armored personnel carrier that consists of a chassis, idler, sprocket, 5 road-wheels, and 64 track links on each track side (right and left). Figure 5 shows the engagement of the track links with some of the vehicle components, while more details about the road wheel arrangement and the configuration of the suspension system of the tracked vehicle model are shown in Fig. 6. Table 1 shows the inertia properties for all the tracked vehicle model components used in this simulation. More specifications of this vehicle can be obtained from open sources (M113, 2003). The vehicle has a suspension system that consists of road arms placed between the road wheels and chassis as well as shock absorbers connected to each road

arm. Table 2 shows the stiffness and the damping coefficients of the contact models used. In this study, two different simulation scenarios, one with the suspension system and the other without the suspension system, will be considered to study the effect of using the suspension system on the results. The road arms and the sprockets are connected to the chassis by revolute joints, and the road arms are connected to the road-wheels by revolute joints. The track links are connected to each other using revolute joints, which can be modeled using the constraint equations, penalty method, bushing element, or ANCF finite elements as previously mentioned. Tensioners are added to the system by connecting each idler to a tensioner with a revolute joint and connecting the tensioner to the chassis with a prismatic joint to ensure only translation between them. The angular velocities of the sprockets of the vehicle model considered in this numerical investigation are assumed to increase after 1 sec until they reach a constant value of 25 rad/sec after 8 seconds as shown in Fig. 7. Figure 8 shows the chassis vertical displacement using the joint model with and without the suspension system. The results presented in this figure show that the model with a suspension system allows for more vibration (a 7 cm initial drop compared to 0.64 cm), which helps make the model more realistic as compared to the previously unsuspended model. The ANCF finite element for the track links used in this investigation is a three-dimensional steel cable element with a modulus of rigidity of 76.9 GPa, a Young's modulus of 200 GPa, and a mass density of 7.80×10^{3} kg/m^{3}. Figures 9 and 10 show, respectively, the chassis forward position and velocity results obtained using different joint models. While the results presented in these figures show good agreement, the computational time varies when these different models are used. The constrained joint model takes less computational time compared to the penalty, bushing element, and ANCF joint models; the

penalty model CPU time is six times that of the constraint model CPU time, while the bushing model CPU time is three times, and the ANCF joint model CPU time is 5 times that of the constraint model CPU time. This increase in the penalty and bushing element CPU time is attributed to the high stiffness coefficients used in both of these models. Efforts are currently being made to improve the efficiency of the ANCF model. Figure 11 shows the motion trajectory of a track link in the chassis coordinate system using the constraint model, the penalty model, the bushing element model, and the ANCF joint model, respectively. The results in this figure show good, although not exact, agreement between the different models. Figures 12 - 15 show the joint forces in the longitudinal and the vertical directions, respectively, obtained using the constrained, penalty, and ANCF joint models. Very high frequencies were filtered out in all models using a low pass FFT with a cut-off frequency of 30 Hz in order to show clearly the nominal values of the joint forces presented in Figs. 12b and 13b. The results presented in these figures are obtained using a stiffness coefficient of 1×10^{9} N/m and damping coefficient of 1×10^{5} N.s/m for the penalty method model. The results show good agreement between the constrained and penalty joint models with the ANCF joint model, as expected, showing lower force magnitude due to the flexibility of the elements. Figures 14 and 15 show the same results in the case of a stiffness coefficient of 1×10^{7} N/m and damping coefficient of 1×10^{5} N.s/m for the penalty method model. The results of Figs. 14 and 15, which show significant differences between the two ideal joint models, demonstrate the drawback of the penalty method when the penalty stiffness coefficient is reduced. Similar results can be expected in the case of the bushing element models where the forces obtained also depend on the stiffness and damping coefficient of the joint. Figure 16 shows the joint deformation predicted using the penalty model using different

stiffness coefficients. The penalty model with a stiffness coefficient of 1×10^9 N/m shows much less deformation, less than 0.075 mm, while the penalty model with a stiffness of 1×10^7 N/m has much more deformation, over 1.5 mm, between the track links.

10. SUMMARY AND CONCULSIONS

In this investigation, different MBS joint formulations are presented and compared using detailed tracked vehicle models. Three main joint formulations are discussed; they are the ideal joint formulation, the compliant discrete element joint formulation, and the compliant continuum-based joint formulation. The ideal joint formulation is developed to eliminate the relative displacement between the two bodies connected by the joint. This can be achieved by enforcing a set of joint algebraic equations using a constrained dynamics approach or by using the penalty method. The constrained dynamics approach eliminates degrees of freedom and ensures that the constraint equations are satisfied at the position, velocity, and acceleration levels. The penalty method, on the other hand, does not reduce the number of degrees of freedom and ensures that the constraint equations are satisfied at the position level only provided that a high stiffness coefficient is used. The compliant discrete element formulation, which allows for joint deformations, can be systematically applied using a standard MBS bushing element that allows for six degrees of freedom of relative motion. The compliant continuum-based approach can be used to develop new joints that capture deformation modes that are not captured by the compliant discrete element joint formulation. ANCF finite elements can be used to systematically develop new joints with distributed elasticity and linear connectivity conditions.

As discussed in this paper, it is important to choose the proper stiffness and damping coefficients when the penalty method and the bushing elements are used. Numerical results were presented in order to compare between different methods. The ideal joint formulation produces the desired joint kinematics and accurate joint forces. The same is true with the penalty force based joint when large penalty stiffness coefficients are used. Penalty force based joint construction has been shown to be sensitive to the selection of penalty stiffness with the higher stiffness coefficients leading to better overall results. However, higher penalty stiffness increases CPU time significantly due to higher frequencies. The penalty method and bushing element models each have much larger CPU times than the ideal constrained model due to these high stiffness coefficients. The results presented in this investigation show that the ANCF joint model leads to lower force predictions which can be attributed to the track link flexibility.

Acknowledgment

This research was supported by the U.S. Army Tank-Automotive Research, Development and Engineering Center (TARDEC) (Contract No. W911NF-07-D-0001).

REFERENCES

1. Bando, K., Yoshida, K., and Hori, K., 1991, "The development of the rubber track for small size bulldozers," *International Off-Highway & Powerplants Congress & Exposition*, Milwaukee, WI.
2. Choi J. H., Lee H. C., and Shabana A. A., 1998, "Spatial Dynamics of Multibody Tracked Vehicles," *Vehicle System Dynamics*, Vol. 29, pp. 27–49.
3. Galaitsis, A. G., 1984, "A Model for Predicting Dynamic Track Loads in Military Vehicles," *Transactions of the ASME, Journal of Vibration, Acoustics, Stress, and Reliability in Design*, Vol. 106, pp. 286-291.
4. Gerstmayr, J. and Shabana, A. A., 2006, "Analysis of Thin Beams and Cables Using the Absolute Nodal Coordinate Formulation," *Nonlinear Dynamics*, Vol. 45, pp. 109-30.
5. "M113," Image, *A Troop 4/12 CAV*, 2003, Web, 11 July 2012, *http://www.atroop412cav.com/tools/ACAV/images/M113-drawing.gif*
6. "M113 Vehicle Family Rubber Track Installation Instructions," *Litho'd in Canada*, 2003, Web, 16 July 2012, <*www.combatreform.org/SoucyBandTrackInstallationA-654RB.pdf*>.
7. Murray, M. and Canfield, T. R., 1992, "Modeling of a flexible link power transmission system," *Proceedings of the 6th ASME International Power Transmission and Gearing Conference*, Scottsdale, Arizona.
8. Nakanishi, T., and Shabana, A. A., 1994, "Contact forces in the nonlinear dynamic analysis of tracked vehicles," *International Journal for Numerical Methods in Engineering*, Vol. 37, pp. 1251-1275.

9. Ozaki, T., and Shabana, A. A., 2003, "Treatment of Constraints in Multibody Systems Part I: Methods of Constrained Dynamics," *Journal of Multi-Scale Computational Engineering*, Vol. 1, pp. 235-252.
10. Ozaki, T. and Shabana, A. A., 2003, "Treatment of Constraints in Multibody Systems, Part II: Application to Tracked Vehicles" *Journal of Multi-Scale Computational Engineering*, Vol. 1, pp. 253-276.
11. Roberson, R. E., and Schertassek, Richard, 1988, *Dynamics of Multibody Systems*, Springer-Verlag, Berlin.
12. Rubinstein, D., Hitron, R., 2004, "A detailed multi-body model for dynamic simulation of off-road tracked vehicles," *Journal of Terramechanics*, Vol. 41, pp. 163–173.
13. Ryu, H. S., Bae, D. S., Choi, J. H., and Shabana, A. A., 2000, "A compliant track link model for high-speed, high-mobility tracked vehicles," *International Journal for Numerical Methods in Engineering*, Vol. 48, pp. 1481-1502.
14. Ryu, H. S., Huh, K. S., Bae, D. S., and Choi, J. H. 2003, "Development of a Multibody Dynamics Simulation Tool for Tracked Vehicles Part I: Efficient Contact and Nonlinear Dynamics Modeling," *JSME International Journal*, **46**(2), pp. 540-549.
15. Shabana, A. A., Zaazaa, K. E., and Sugiyama, Hiroyuki, 2008, *Railroad Vehicle Dynamics: A Computational Approach*, Taylor & Francis/CRC, Boca Raton, Florida.
16. Shabana, A. A., Hamed, A. M., Mohamed, A. A., Jayakumar, P., and Letherwood, M. D. 2012, "Use of B-Spline in the Finite Element Analysis: Comparison with ANCF Geometry," *Journal of Computational and Nonlinear Dynamics*, Vol. 7, pp. 81-88.

17. Yakoub, R. Y., and Shabana, A. A., 2001, "Three Dimensional Absolute Nodal Coordinate Formulation for Beam Elements: Implementation and Application," *ASME Journal for Mechanical Design*, Vol. 123, pp. 614–621.

Table 1: Mass and inertia values for tracked vehicle parts

Part	Mass (kg)	I_{XX} (kg.m^2)	I_{YY} (kg.m^2)	I_{ZZ} (kg.m^2)	I_{XY}, I_{YZ}, I_{XZ} (kg.m^2)
Chassis	5489.2	1786.9	10450	10721	0
Sprocket	436.67	13.868	12.216	12.216	0
Idler	429.57	14.698	12.545	12.545	0
Road Wheel	561.07	26.063	19.819	19.819	0
Road Arm	75.264	0.77085	0.37632	0.77085	0
Track Link	18.024	0.04113	0.22463	0.25256	0

Table 2: Contact Parameters

Parameters	Sprocket-Track Contact	Road Wheel-Track Contact	Ground-Track Contact
k	2.00×10^6 N/m	2.00×10^6 N/m	2.00×10^6 N/m
c	5.00×10^3 N·s/m	5.00×10^3 N·s/m	5.00×10^3 N·s/m
μ	0.150	0.100	0.300

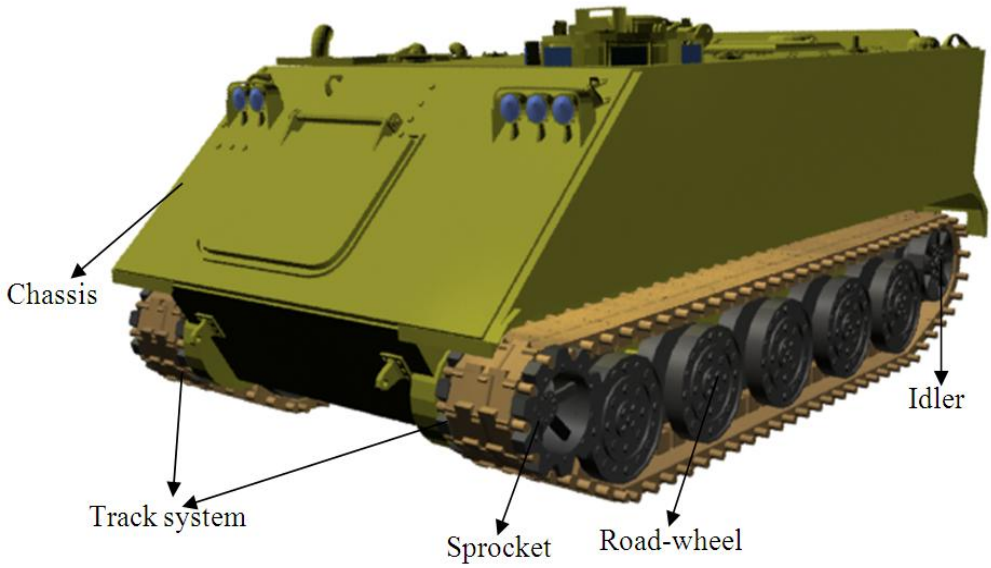

Figure 1: The SAMS/2000 tracked vehicle model

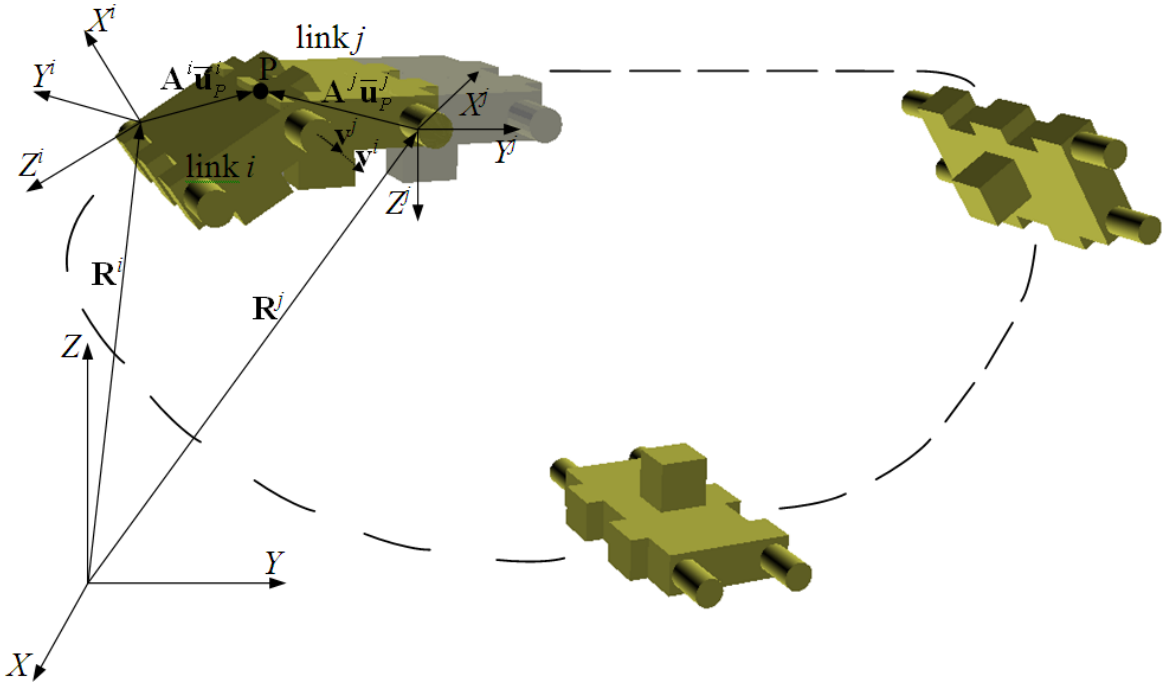

Figure 2: Revolute joint

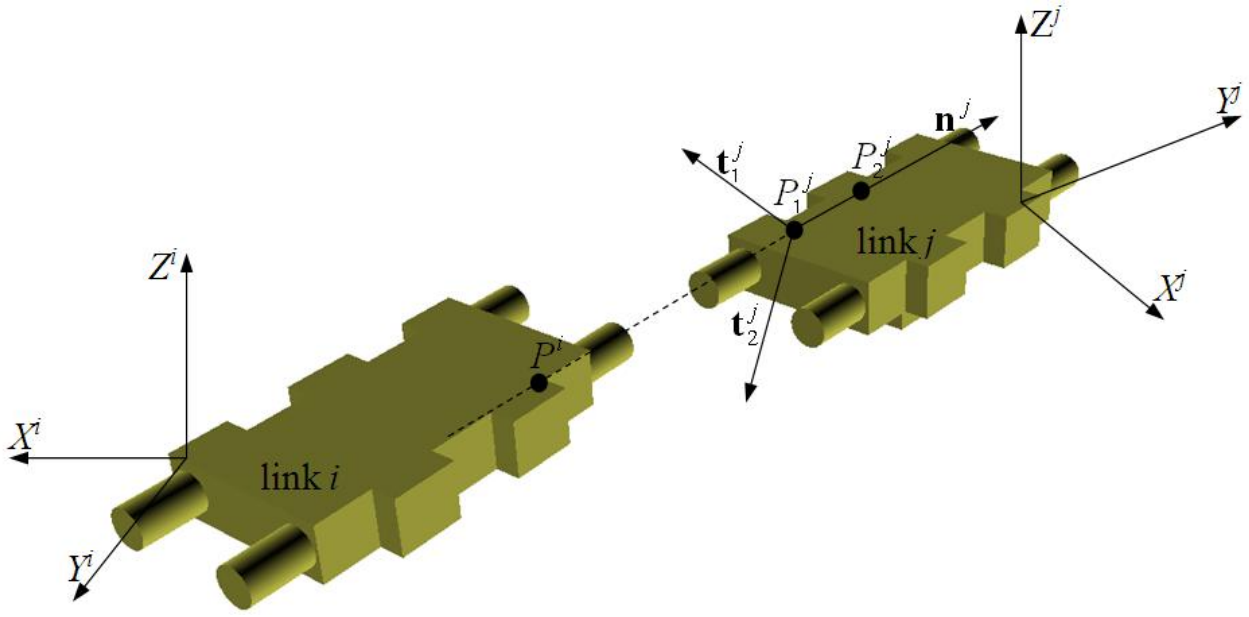

Figure 3: Bushing element

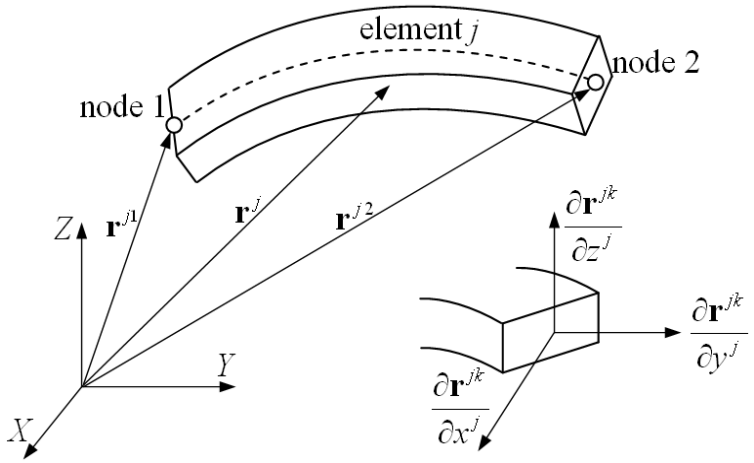

Figure 4: ANCF beam element coordinates

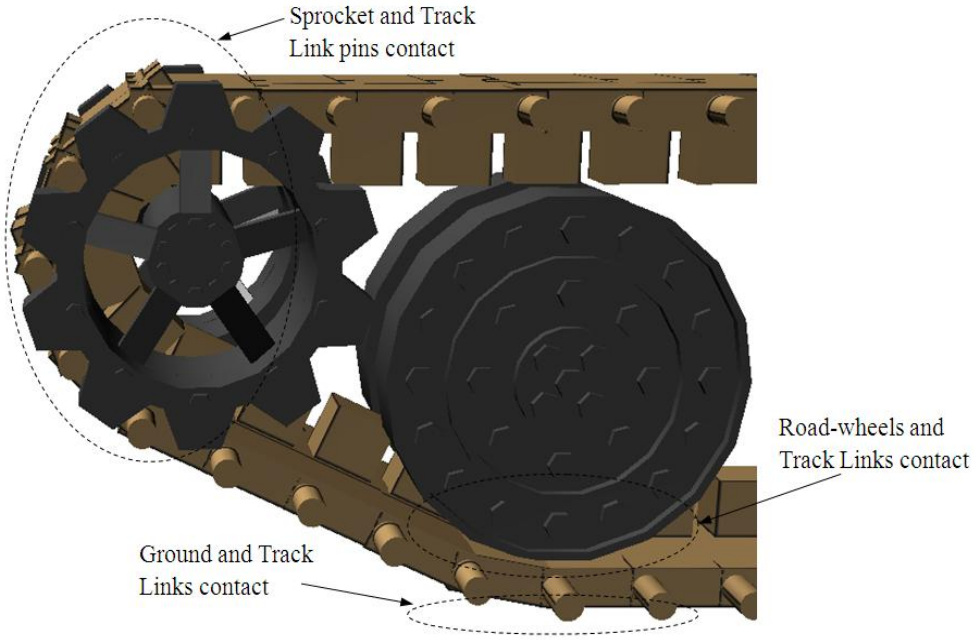

Figure 5: Tracked vehicle contact models

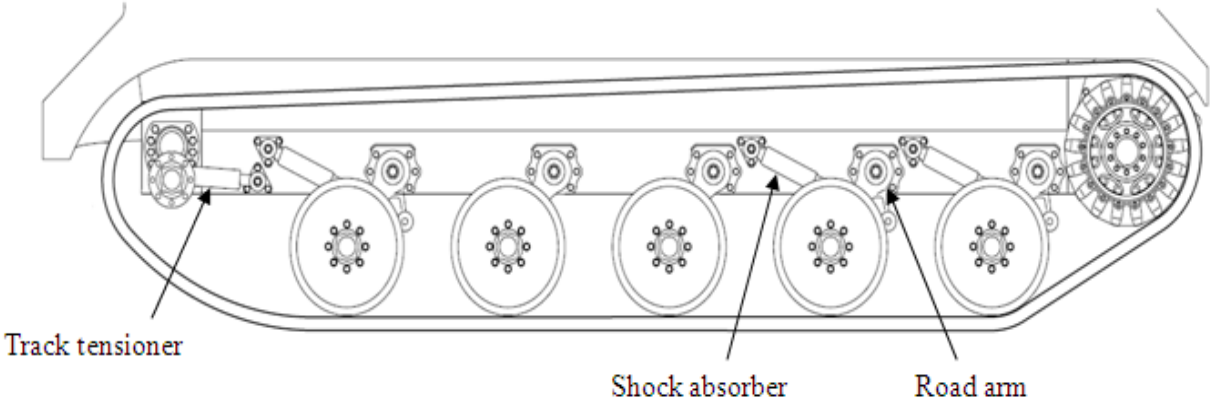

Figure 6: Suspension system layout of the tracked vehicle
(www.combatreform.org/SoucyBandTrackInstallationA-654RB.pdf)

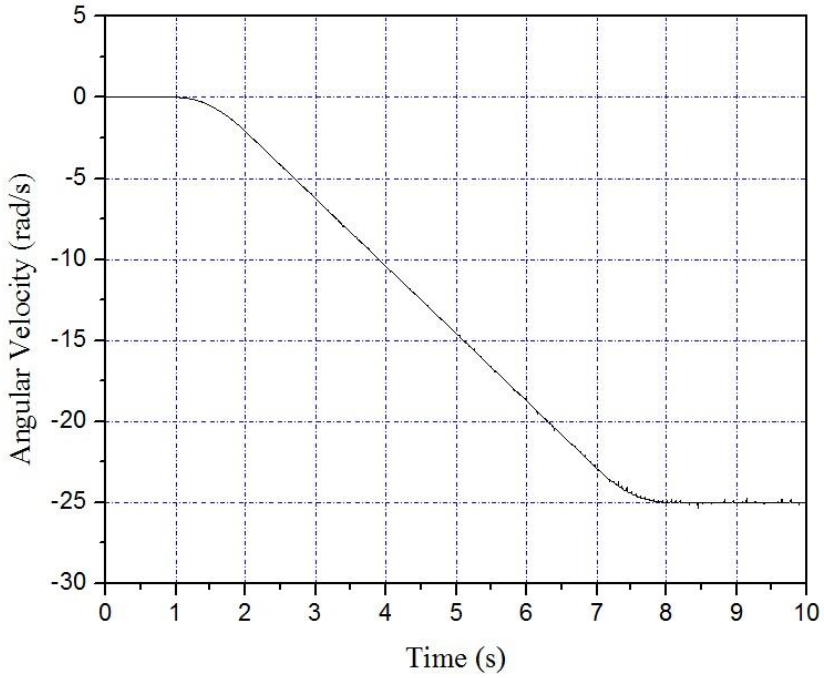

Figure 7: Sprocket angular velocity

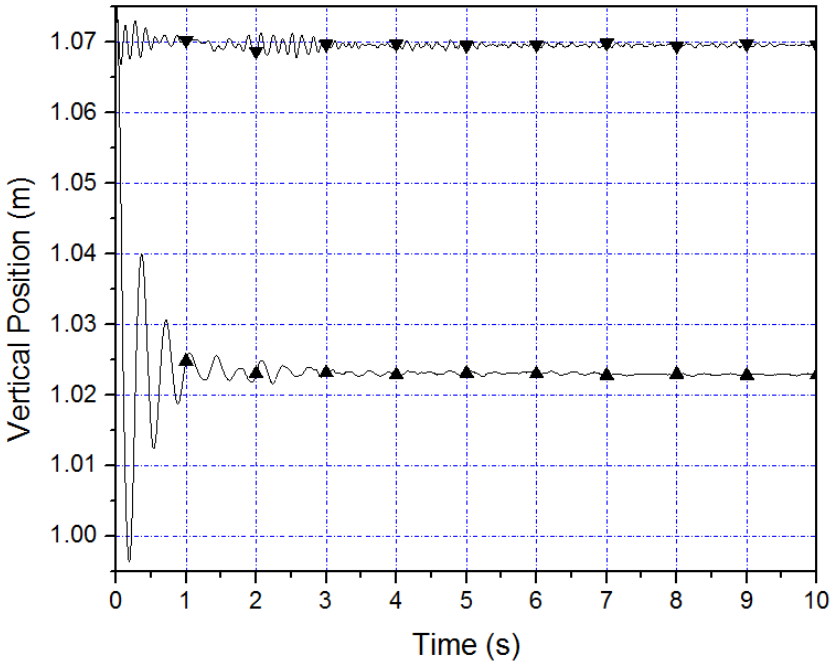

Figure 8: Chassis vertical displacement
(—▲— with suspension, —▼— without suspension)

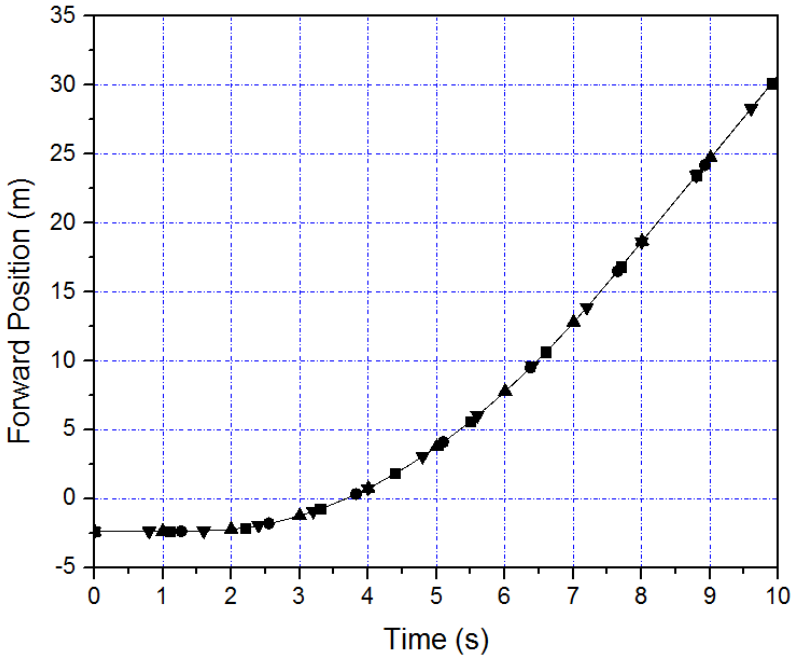

Figure 9: Chassis forward position
(—▲— Constrained joint model, —▼— Penalty method model, —■— Bushing element model, —●— ANCF model)

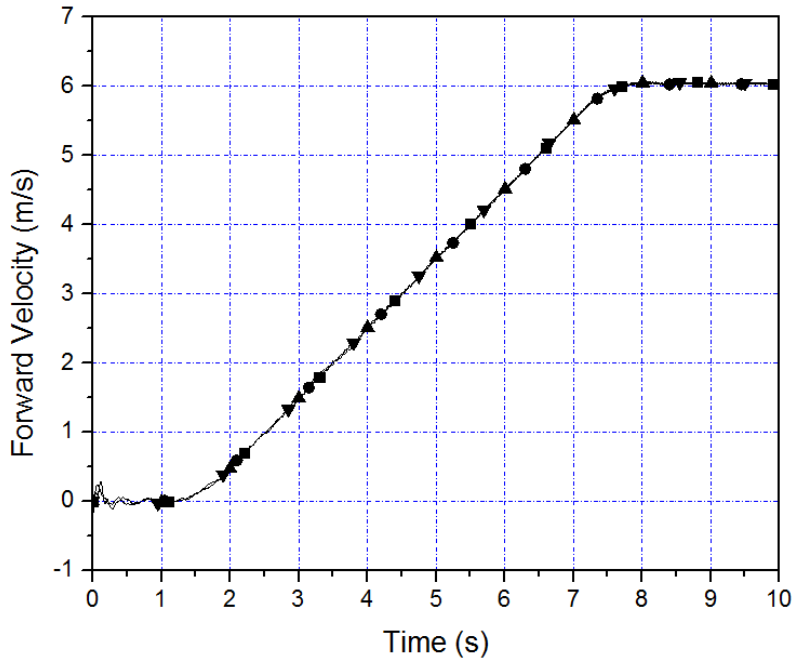

Figure 10: Chassis forward velocity
(—▲— Constrained joint model, —▼— Penalty method model, —■— Bushing element model, —●— ANCF model)

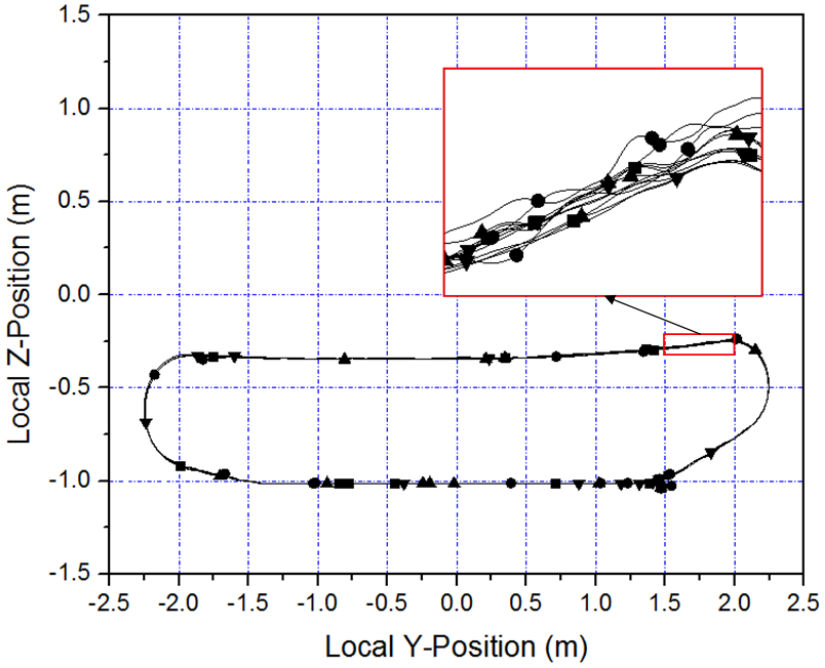

Figure 11: Trajectory motion of a track link in the chassis coordinate system
(—▲— Constrained joint model, —▼— Penalty method model, —■— Bushing element model, —●— ANCF model)

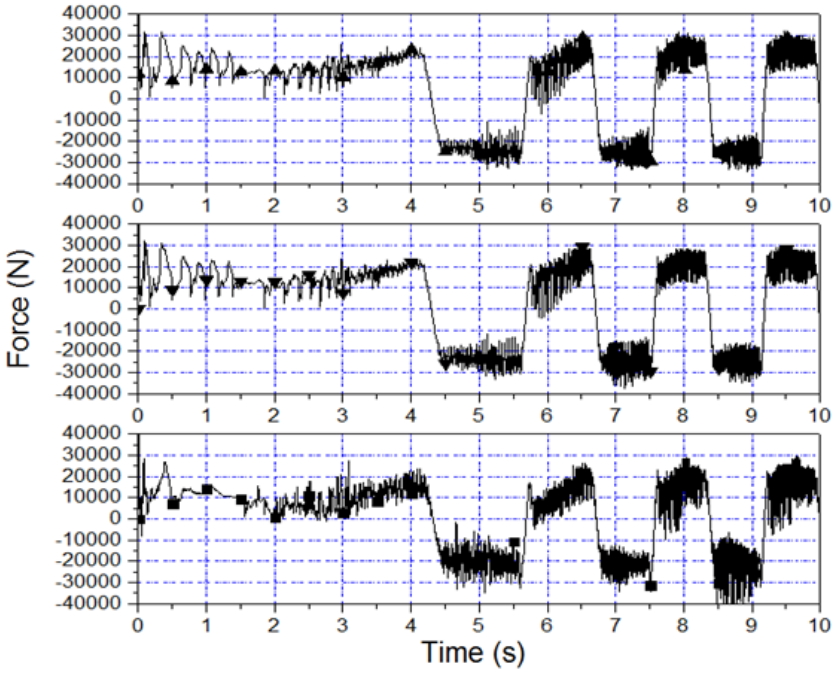

Figure 12a: Joint longitudinal forces
(—▲— Constrained joint model, —▼— Penalty method model k = 1×10^{9} N/m, —■— ANCF model)

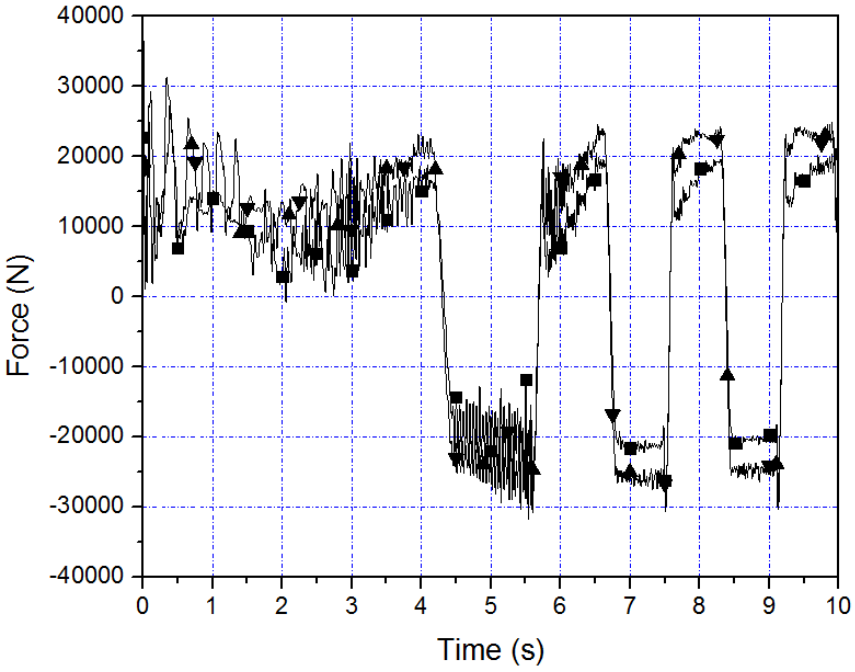

Figure 12b: Filtered joint longitudinal forces using FFT
(—▲— Constrained joint model, —▼— Penalty method model k = 1×10^{9} N/m, —■— ANCF model)

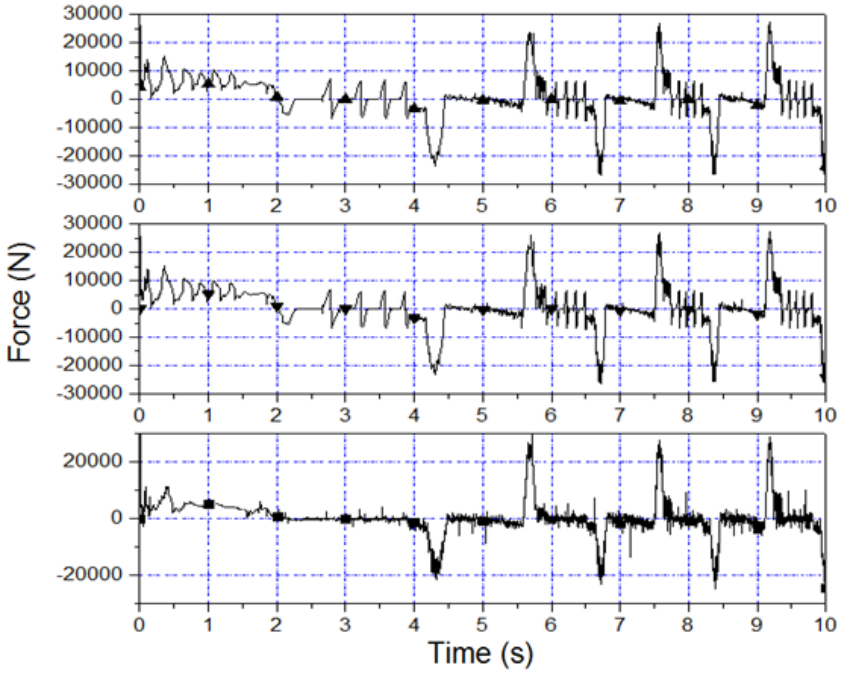

Figure 13a: Joint vertical forces
(—▲— Constrained joint model, —▼— Penalty method model k = 1×10^{9} N/m, —■— ANCF model)

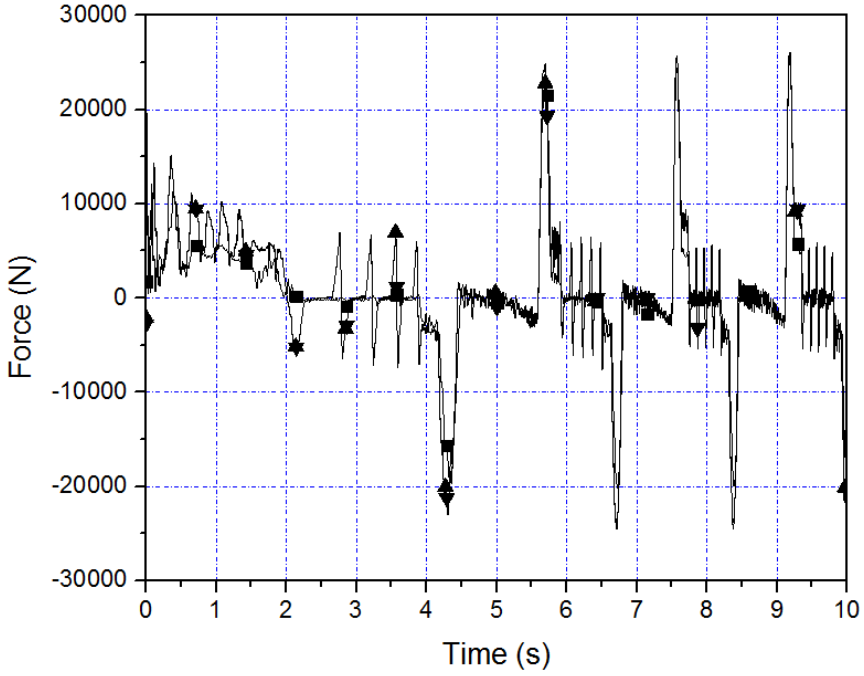

Figure 13b: Filtered joint vertical forces using FFT
(—▲— Constrained joint model, —▼— Penalty method model k = 1×10^{9} N/m, —■— ANCF model)

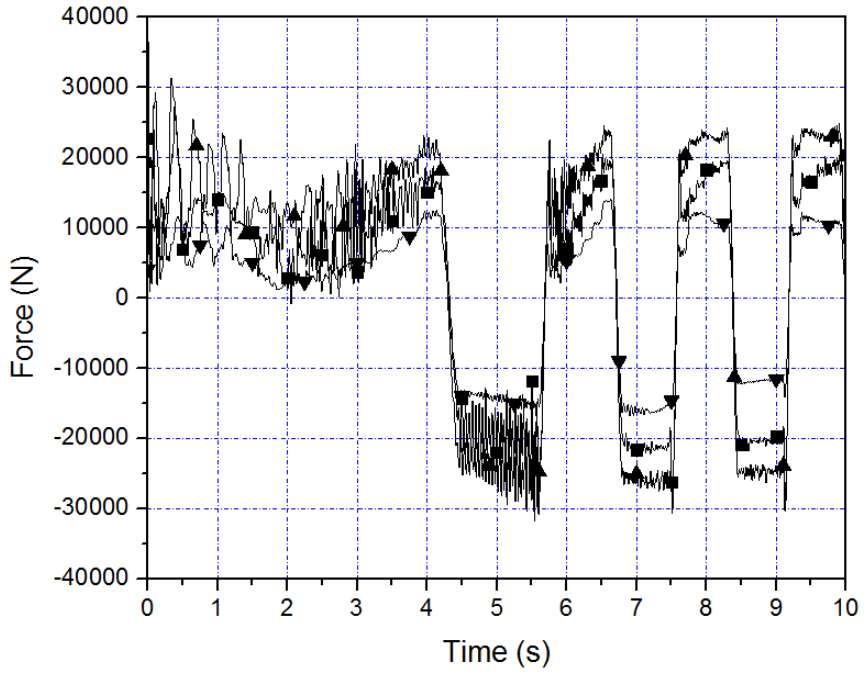

Figure 14: Joint Longitudinal forces
(—▲— Constrained joint model, —▼— Penalty method model k = 1×10^{7} N/m, —■—ANCF model)

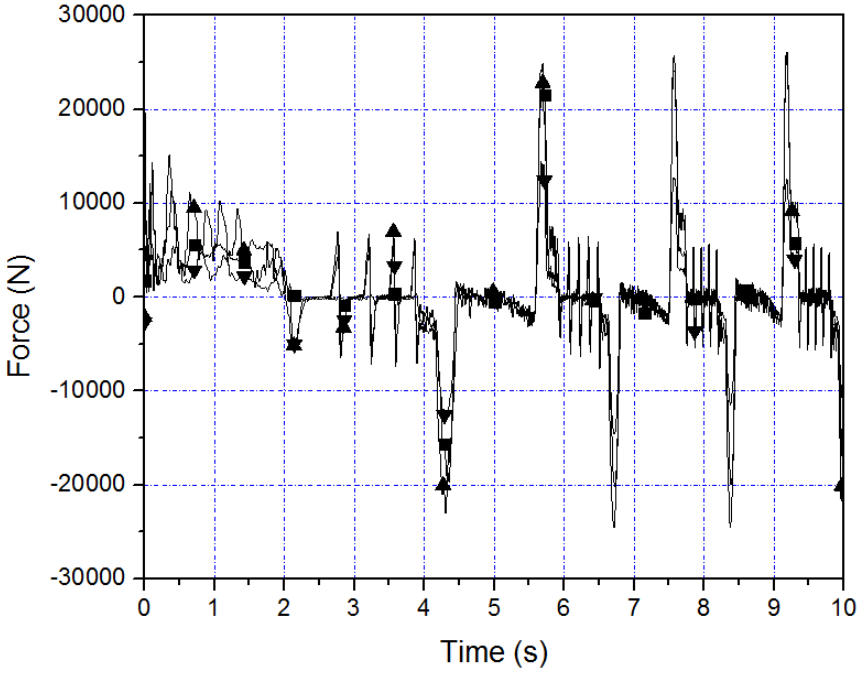

Figure 15: Joint vertical forces
(—▲— Constrained joint model, —▼— Penalty method model k = 1×10^{7} N/m, —■— ANCF model)

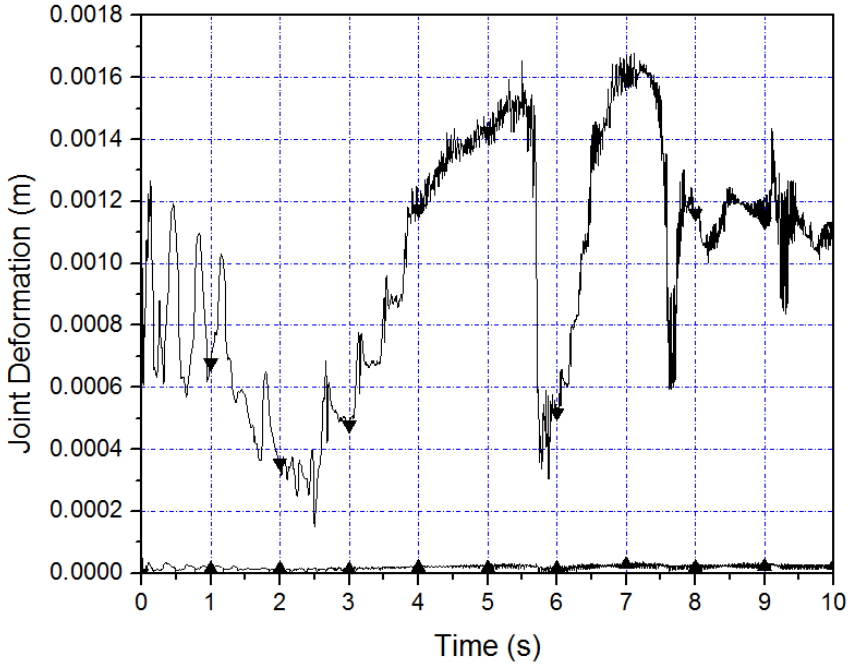

Figure 16: Joint deformation using penalty model
(—▲— k = 1×10^{9} N/m, —▼— k = 1×10^{7} N/m)